Liquid Crystals
Publication details, including instructions for authors and subscription information:
http://www.informaworld.com/smpp/title~content=t713926090

Orientation of mesophase pitch in capillary and channel flows

John J. McHugh[a]; Dan D. Edie[a]
[a] Department of Chemical Engineering and Center for Advanced Engineering Fibers, Clemson University, Clemson, South Carolina, U.S.A.

To cite this Article McHugh, John J. and Edie, Dan D.(1995) 'Orientation of mesophase pitch in capillary and channel flows', Liquid Crystals, 18: 2, 327 — 335
To link to this Article: DOI: 10.1080/02678299508036629
URL: http://dx.doi.org/10.1080/02678299508036629

LIQUID CRYSTALS, 1995, VOL. 18, NO. 2, 327–335

Orientation of mesophase pitch in capillary and channel flows

by JOHN J. McHUGH and DAN D. EDIE*
Department of Chemical Engineering and Center for Advanced Engineering Fibers, Clemson University, Earle Hall, Box 340909, Clemson, South Carolina 29634-0909, U.S.A.

(Received 10 December 1993; accepted 1 April 1994)

Analytical solutions to the Leslie–Ericksen equations are discussed for flow through a circular capillary and a rectangular channel. The analysis allows for a director component out of the flow–gradient plane. The resulting orientation profiles match the commonly observed textures of mesophase pitch-based carbon fibres, specifically the radial and line-origin textures. Thus, this formulation would appear to be correct for the flow of discotic mesophase pitches. Furthermore, the velocity profile for capillary flow suggests the possibility of measuring the Leslie coefficient α_4 for a mesophase pitch using a capillary rheometer.

1. Introduction

The physical properties of high-performance fibres are largely a result of the molecular orientation created during the fibre forming process. Since liquid crystalline materials will orient under shear flow, most of these fibres are formed from liquid crystalline, or mesophase, precursors. In such processes, orientation is achieved as the fibres pass through spinnerette capillaries. Fibre drawing merely accentuates orientation parallel to the fibre axis. Examples of liquid crystalline polymers that can form high-performance fibres include Kevlar® (poly (*p*-phenylene terephthalamide)), liquid crystal polyesters, and PBO (poly (*p*-phenylene benzobisoxazole)).

A relatively new class of high-performance carbon fibres is melt-spun from mesophase pitch, a discotic nematic liquid crystalline material. This variety of carbon fibres is unique in that it can develop extended graphitic crystallinity during carbonization, in contrast to carbon fibres produced from polyacrylonitrile (PAN).

The mesophase pitches used for high-modulus carbon fibre production can be formed either by the thermal polymerization of petroleum- or coal tar-based pitches [1, 2] or by the catalytic polymerization of pure compounds such as naphthalene [3]. The mesophase transformation was discovered by Brooks and Taylor [4] as an intermediate phase, formed between 400°C and 550°C, during the thermal treatment of aromatic hydrocarbons. During mesophase formation, domains of highly parallel, plate-like molecules form and coalesce until, with time, a 100 per cent anisotropic material may be obtained. It has been well-established that, when mesophase pitch is carbonized, the morphology of the pitch is the primary factor [5] in determining the microstructure of the resulting graphitic material.

This relationship between the melt orientation of mesophase pitch and the texture of the carbonized fibres accounts for the unique properties attainable in this class of fibre. When mesophase pitch is melt-spun into fibre form, there is very strong axial alignment of the aromatic rings caused by the shear field through the capillaries and subsequent fibre drawing. This orientation is critical in determining the properties of the carbonized fibres, as there is extreme anisotropy in the mechanical and transport of graphite.

In addition to excellent mechanical properties, mesophase pitch-based carbon fibres can develop thermal conductivities as high as five times that of copper and orders-of-magnitude higher than PAN-based carbon fibres, approaching the value of single crystal graphite. The high thermal conductivity of graphite is due to excellent lattice wave conduction along the basal planes. Therefore, when developing a high thermal conductivity fibre, it is essential that the fibre possess extended graphitic domains. In addition to strong axial orientation, it is critical that the spacing between the basal planes within the fibre is minimized to enhance thermal conductivity. Hence, on a microscopic level, forming a fibre with a highly linear transverse texture is very important in developing thermal conductivity.

The melt-spinning of mesophase pitch through non-circular capillaries offers the possibility of altering transverse orientation and producing a more parallel structure [6]. However, any attempt to optimize the

* Author for correspondence.

structure of carbon fibres formed from mesophase pitch requires a fundamental understanding of the flow behaviour of this unique material. In this regard, modelling of mesophase pitch using available liquid crystal continuum theory is a logical starting point. However, applying this approach to mesophase pitch will, inevitably, involve approximations. First, mesophase pitch consists of a wide range of species, and therefore, one must realize that only the average molecular shape is discotic. Also, mesophase pitch is opaque, its composition may change with time above its softening point, and its liquid crystalline temperature region is typically around 300°C. These factors make a complete evaluation of its viscosity coefficients and elastic constants impractical. However, in spite of these difficulties, a qualitative understanding of the development of orientation during the melt-spinning of mesophase pitch is a reasonable goal. Furthermore, such an approach is necessary to optimize the structure-dependent properties of mesophase pitch-based carbon fibres.

2. Theory

The flow behaviour of nematic liquid crystals is much more complex than that of conventional fluids. This is due to the coupling between molecular orientation and fluid flow. Normally, the molecular orientation of nematics is quantified by a unit vector $\mathbf{n}$, which points in the direction around which the molecules possess rotational symmetry. This implies that, for liquid crystals consisting of disk-like molecules, the director defines the *short* molecular axis.

The fluid mechanics of nematic liquid crystals is described by the theory proposed by Leslie [7, 8] and Ericksen [9–12]. In this analysis, three equations, namely the conservation of mass, linear momentum, and angular momentum, describe the relationship between the pressure P, the local velocity $\boldsymbol{v}$, and the director.

2.1. *Conservation of mass*

As with isotropic fluids, the conservation of mass equates the mass accumulation within a system to the bulk mass flow into the system,

$$\frac{\partial \rho}{\partial t} = -(\nabla \cdot \rho \boldsymbol{v}), \tag{1}$$

where ρ is the density. To simplify matters, the assumption of fluid incompressibility is employed, $\rho \neq \rho(\mathbf{r}, t)$ ($\mathbf{r}$ is the position vector), simplifying equation (1) to

$$(\nabla \cdot \boldsymbol{v}) = 0. \tag{2}$$

2.2. *Conservation of linear momentum*

The most general form of the conservation of linear momentum for nematic mesophases is

$$\rho \frac{\partial \boldsymbol{v}}{\partial t} = -\rho(\boldsymbol{v} \cdot \nabla)\boldsymbol{v} - \nabla P + [\nabla \cdot \boldsymbol{\sigma}], \tag{3}$$

where $\boldsymbol{\sigma}$ is the stress tensor, expressible as the sum of viscous and distortion terms

$$\sigma_{ij} = \tau_{ij} - \sum_k \frac{\partial F}{\partial(\partial n_k/\partial x_i)} \frac{\partial n_k}{\partial x_j}, \tag{4}$$

where F is the free energy density (described below). The distortion term normally is much smaller than the viscous term and shall be neglected in the following analysis. In such cases, equation (3) becomes

$$\rho \frac{\partial \boldsymbol{v}}{\partial t} = -\rho(\boldsymbol{v} \cdot \nabla)\boldsymbol{v} - \nabla P + [\nabla \cdot \boldsymbol{\tau}]. \tag{5}$$

For isotropic (newtonian) fluids, the viscous stress tensor would simply be proportional to the rate of deformation tensor, $\mathbf{A}$, where the constant of proportionality is the fluid viscosity, η. Leslie postulated that the viscous stress tensor for nematics should be equal to the sum of six terms, each multiplied by a distinct 'viscosity'. The non-symmetric Leslie viscous stress tensor was developed as the most general form expressing a linear dependence on the rate of deformation and the director motion vector, which represents the rate of change of the director relative to the background rotation of the continuum. The Leslie coefficients represent the resistance to different kinds of viscous deformation. For instance, α_4 relates to a material's resistance to simple shear flow (the only non-zero coefficient for an isotropic material). The Leslie viscous stress tensor is defined as

$$\begin{aligned} \boldsymbol{\tau} = {} & \alpha_1 \mathbf{n}(\mathbf{n} \cdot [\mathbf{A} \cdot \mathbf{n}])\mathbf{n} + \alpha_2 \mathbf{n}\mathbf{N} + \alpha_3 \mathbf{N}\mathbf{n} + \alpha_4 \mathbf{A} \\ & + \alpha_5 \mathbf{n}[\mathbf{n} \cdot \mathbf{A}] + \alpha_6 [\mathbf{n} \cdot \mathbf{A}]\mathbf{n}. \end{aligned} \tag{6}$$

The rate of deformation tensor and the director motion vector, $\mathbf{N}$, may be written as

$$\mathbf{A} = \tfrac{1}{2}([\nabla \boldsymbol{v}] + [\nabla \boldsymbol{v}]^{\mathrm{T}}), \tag{7}$$

$$\mathbf{N} = \frac{\partial \mathbf{n}}{\partial t} + (\boldsymbol{v} \cdot \nabla)\mathbf{n} - [\boldsymbol{\omega} \times \mathbf{n}], \tag{8}$$

where $\boldsymbol{\omega}$ is the vorticity vector, defined as

$$\boldsymbol{\omega} = \tfrac{1}{2}[\nabla \times \boldsymbol{v}]. \tag{9}$$

Through a relation developed by Parodi [13],

$$\alpha_6 - \alpha_5 = \alpha_2 + \alpha_3, \tag{10}$$

only five Leslie coefficients are actually independent. The five independent coefficients can be related to five measurable quantities: the measured viscosities with the director externally fixed (for example, by a magnetic field) in the flow, gradient, neutral, and 45° (within the flow–gradient plane) directions, and the optically measured shear-alignment angle (in the absence of external fields).

2.3. *Conservation of angular momentum*

The conservation of angular momentum requires that the accumulation of angular momentum within a system equals the sum of the torques that act upon the system. In nematic liquid crystals, such torques can arise from elastic or viscous deformations. Thus,

$$I\frac{D\mathbf{\Omega}}{Dt} = \mathbf{\Gamma}_{\text{elas}} + \mathbf{\Gamma}_{\text{visc}}, \tag{11}$$

where I is the moment of inertia and $\mathbf{\Omega}$ is a local angular velocity of the director, defined by

$$\mathbf{\Omega} = \left[\mathbf{n} \times \left[\frac{\partial \mathbf{n}}{\partial t} + (\boldsymbol{v}\cdot\nabla)\mathbf{n}\right]\right]. \tag{12}$$

At moderate rotational velocities, the accumulation term is very small. Thus, if this term is neglected, the elastic and viscous torques must balance, or

$$\mathbf{\Gamma}_{\text{elas}} + \mathbf{\Gamma}_{\text{visc}} = 0. \tag{13}$$

The elastic torque, $\mathbf{\Gamma}_{\text{elas}}$, is handled through analogy with the linear elastic theory of solids, where restoring forces oppose strains. In nematics, curvature of an initially (and uniformly) oriented liquid crystal is opposed by a restoring torque. Furthermore, analogous to Hooke's law, these 'torque stresses' are assumed to be proportional to the curvature strains [$\partial n_x/\partial x$, $\partial n_x/\partial y$, etc.). This implies that the free energy density is proportional to the square of the curvature strains, where the total free energy relative to the state of uniform orientation is the volume integral of this free energy density. Based on earlier work by Oseen [14], Frank [15] derived the following expression for the Helmholtz free energy density, F, of nematic liquid crystals

$$F = \tfrac{1}{2}[K_1(\nabla\cdot\mathbf{n})^2 + K_2(\mathbf{n}\cdot\nabla\times\mathbf{n})^2 + K_3[\mathbf{n}\cdot\nabla\mathbf{n}]\cdot[\mathbf{n}\cdot\nabla\mathbf{n}]]. \tag{14}$$

The constants, K_1, K_2, and K_3 are called Oseen–Frank constants and relate to the splay, twist, and bend modes of deformation, respectively. A common assumption that greatly simplifies the mathematics is to set the elastic constants equal. In this case, equation (14) becomes

$$F = \tfrac{1}{2}K[(\nabla\cdot\mathbf{n})^2 + [\nabla\times\mathbf{n}]^2\cdot[\nabla\times\mathbf{n}]]. \tag{15}$$

Subject to the constraint, $(\mathbf{n}\cdot\mathbf{n}) = 1$, if the total free energy is minimized with respect to all changes in orientation, the following equilibrium relationship results:

$$-\frac{\partial F}{\partial n_i} + \sum_j \frac{\partial}{\partial x_j}\left[\frac{\partial F}{\partial(\partial n_i/\partial x_j)}\right] = -\lambda(\mathbf{r})n_i, \tag{16}$$

where λ, a Lagrange multiplier, is an arbitrary function of position, $\mathbf{r}$. The left-hand side of equation (16) is defined as the molecular field, h_i. Condition (16) states that, at equilibrium, the molecular field must be parallel to the director (because λ is a scalar). If $\mathbf{h}$ is not parallel to $\mathbf{n}$, the elastic torque is non-zero and is given by

$$\mathbf{\Gamma}_{\text{elas}} = \mathbf{n}\times\mathbf{h}. \tag{17}$$

Differentiation of the expression for free energy density, equation (14), yields the following relation for the molecular field:

$$\begin{aligned}\mathbf{h} = {} & K_1\nabla(\nabla\cdot\mathbf{n}) - K_2\{(\mathbf{n}\cdot[\nabla\times\mathbf{n}])[\nabla\times\mathbf{n}] \\ & + \nabla[(\mathbf{n}\cdot[\nabla\times\mathbf{n}])\mathbf{n}\} + K_3\{[\mathbf{n}\times[\nabla\times\mathbf{n}]] \\ & \times[\nabla\times\mathbf{n}] + \nabla\times[\mathbf{n}\times[\mathbf{n}\times[\nabla\times\mathbf{n}]]]\}.\end{aligned} \tag{18}$$

However, if the Oseen–Frank constants are assumed to be equal, equation (18) simplifies to

$$\mathbf{h} = K\nabla^2\mathbf{n}. \tag{19}$$

The viscous torque, like the viscous stress tensor, is described by a constitutive equation,

$$\mathbf{\Gamma}_{\text{visc}} = -\gamma_1[\mathbf{n}\times\mathbf{N}] - \gamma_2[\mathbf{n}\times[\mathbf{A}\cdot\mathbf{n}]]. \tag{20}$$

where γ_1 and γ_2 are the shear-torque coefficients, which are related to the Leslie coefficients by

$$\gamma_1 = \alpha_3 - \alpha_2 \quad\text{and}\quad \gamma_2 = \alpha_2 + \alpha_3. \tag{21}$$

Substitution of equations (17) and (20) into the balance of torques, equation (13), yields

$$[\mathbf{n}\times\mathbf{h}] = \gamma_1[\mathbf{n}\times\mathbf{N}] + \gamma_2[\mathbf{n}\times[\mathbf{A}\cdot\mathbf{n}]]. \tag{22}$$

In short, the above Leslie–Ericksen model contains five independent 'viscosity' coefficients in the stress tensor and three elastic constants in the expression for the free energy. In using the Leslie–Ericksen model, it is assumed that the fluid is incompressible and isothermal. In the following examples, it is also assumed that there are no external torques, that the elastic constants are equal, and that the inertial terms in the equations of motion are negligible.

3. Capillary flow

We begin identically to the analysis of Poiseuille flow of isotropic fluids, assuming that only the axial component of fluid velocity is non-zero, that is

$$v_r = v_\theta = 0, \tag{23}$$

and from the conservation of mass,

$$v_z = v_z(r). \tag{24}$$

In order to write the conservation of angular momentum for capillary flow, we must first characterize the director, $\mathbf{n}$, at any position in space. If we consider a single 'disk' (actually a statistical average of a very large number of molecules) at some arbitrary position in space, the orientation of its director may be completely described by two angles. Let ζ represent the angle between the director and the flow–gradient plane, while β is the angle between the director and the flow axis, as shown in figure 1.

The director components are as follows:

$$n_r = \cos\zeta \sin\beta, \quad n_\theta = \sin\zeta \sin\beta, \quad n_z = \cos\beta. \tag{25}$$

The 'shear-aligning' case where $\zeta = 0°$ has been treated by Atkin [16] and Tseng *et al.* [17], and is reviewed by Leslie [18]. These studies precede any discussion of discotic mesophases, and this form of a solution does not seem to describe the flow behaviour of mesophase pitches. More generally, one could also allow the 'out-of-plane' angle, ζ, to vary with radial position, r.

In this general description, the viscous and elastic torques (equations (20) and (17)) are

$$\boldsymbol{\Gamma}_{\text{visc}} = \begin{Bmatrix} -\dfrac{\alpha_2}{2}\sin(2\zeta)\sin^2\beta\,\dfrac{dv_z}{dr} \\[2ex] (\alpha_2\cos^2\zeta\sin^2\beta - \alpha_3\cos^2\beta)\,\dfrac{dv_z}{dr} \\[2ex] \dfrac{\alpha_3}{2}\sin\zeta\sin(2\beta)\,\dfrac{dv_z}{dr} \end{Bmatrix}, \tag{26}$$

$$\boldsymbol{\Gamma}_{\text{elas}} = \begin{Bmatrix} K\left[-\dfrac{\cos\zeta\sin(2\beta)}{2r}\dfrac{d}{dr}\left(r\dfrac{d\zeta}{dr}\right) - \dfrac{\sin\zeta}{r} \times \dfrac{d}{dr}\left(r\dfrac{d\beta}{dr}\right) + \dfrac{\sin\zeta\sin(2\beta)}{2}\left(\dfrac{d\zeta}{dr}\right)^2 - 2\cos\zeta\cos^2\beta\,\dfrac{d\zeta}{dr}\dfrac{d\beta}{dr} + \dfrac{\sin\zeta\sin(2\beta)}{2r^2}\right] \\[3ex] K\left[-\dfrac{\sin\zeta\sin(2\beta)}{2r}\dfrac{d}{dr}\left(r\dfrac{d\zeta}{dr}\right) + \dfrac{\cos\zeta}{r} \times \dfrac{d}{dr}\left(r\dfrac{d\beta}{dr}\right) - \dfrac{\cos\zeta\sin(2\beta)}{2}\left(\dfrac{d\zeta}{dr}\right)^2 - 2\sin\zeta\cos^2\beta\,\dfrac{d\zeta}{dr}\dfrac{d\beta}{dr} - \dfrac{\cos\zeta\sin(2\beta)}{2r^2}\right] \\[3ex] K\left[\dfrac{\sin^2\beta}{r}\dfrac{d}{dr}\left(r\dfrac{d\zeta}{dr}\right) + \sin(2\beta)\dfrac{d\zeta}{dr}\dfrac{d\beta}{dr}\right] \end{Bmatrix}. \tag{27}$$

As mentioned above, there exists one solution within the flow–gradient plane ($\zeta = 0°$) where the torques balance. It may be readily observed that each component of the viscous and elastic torques also vanishes at $\zeta = \beta = 90°$; however, such an out-of-plane solution is generally assumed to be unstable. This is because a perturbation on the angle, ζ, away from this solution ($\zeta = \beta = 90°$) will cause a non-zero viscous torque. The r-component of this torque should tend to rotate the director into the plane of shear, where $\beta = 0°$ (see equation (26) and figure 1).

Quantitatively, if the perturbation on ζ is $90° - \delta$, the r-component of the viscous torque may be written as

$$\Gamma_{\text{visc},r} = \frac{\alpha_2}{2}\sin(2\delta)\left(-\frac{dv_z}{dr}\right)\sin^2\beta, \tag{28}$$

which is positive for $\alpha_2 > 0$. (A positive α_2 is predicted if the nematic molecules are modelled as rigid, oblate ellipsoids of revolution [19, 20].)

If it is assumed that the perturbation on ζ occurs at a given position, r, the r-component of the elastic torque will have one dominant term, namely

$$\Gamma_{\text{elas},r} = -\frac{K}{r}\frac{d}{dr}\left(r\frac{d\beta}{dr}\right). \tag{29}$$

Since the viscous torque due to the perturbation on ζ tends to decrease β, a relative minimum on β at r will result. This implies that the second derivative of β with respect to r is positive and the elastic torque is negative. Therefore, if the orientation is initially near $\zeta = \beta = 90°$, the viscous tendency to rotate the director around the r-axis will be opposed by an elastic torque, for $\alpha_2 > 0$. It seems that the magnitude of the Ericksen number ($\text{Er} = Dv\eta/K$) may be critical in evaluating the stability of out-of-plane orientation with respect to a perturbation of a given magnitude.

If one considers the anchoring behaviour of mesophase pitch, a mechanism for the proximity to the out-of-plane solution can be proposed. (Note that the anchoring of discotic molecules is described by the angle, ζ, in contrast to rod-like nematics, i.e. their long molecule axes are anchored, as opposed to their director.) It has been widely observed that the pitch molecules tend to orient with the aromatic rings perpendicular to many solid surfaces (including stainless steel, the usual material of construction for spinnerettes). This corresponds to a boundary angle, ζ, equal to 90°. Again, under such a configuration, the r-component of torque is responsible for changing the angle, β. With the angle, ζ, equal to 90° at the capillary wall

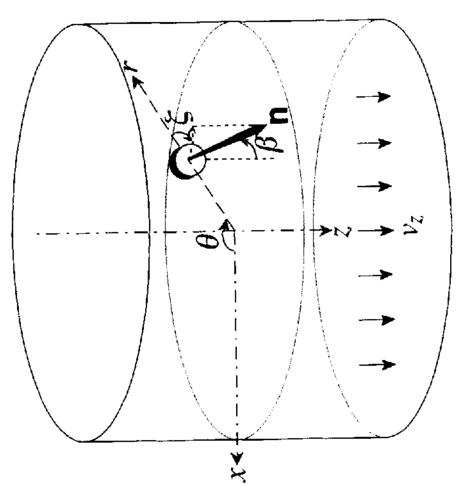

Figure 1. Director orientation angles in cylindrical coordinates.

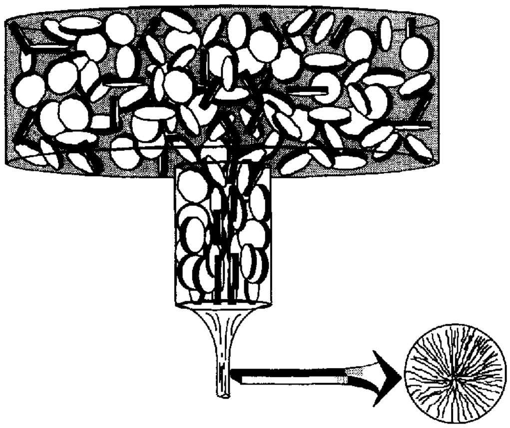

Figure 2. Origin of radial texture in circular mesophase pitch-based carbon fibres.

(where the shear rate is maximum), the viscous torque is zero (or, at least, very small). It may be further argued that entrance effects cause a large β approaching 90°.

The out-of-plane solution suggests a radial orientation of the aromatic planes. From the above result, the origin of the radial texture most commonly found in mesophase pitch-based carbon fibres may be deduced and is illustrated in figure 2. Inspection of the cross-section of a circular mesophase fibre usually shows that the graphite crystallites converge toward the centre of the fibre, as shown schematically in figure 2. Clearly, the disks representing the molecular orientation before and within the capillary should not be considered drawn to scale. Figure 3 shows a scanning electron micrograph (SEM) of the radial texture of a mesophase pitch-based carbon fibre melt-spun from a circular capillary. This radial texture develops when flow is fully developed during extrusion through the spinnerette. Past work has shown that this texture of mesophase pitch-based carbon fibres is a direct reflection of the molecular structure [22].

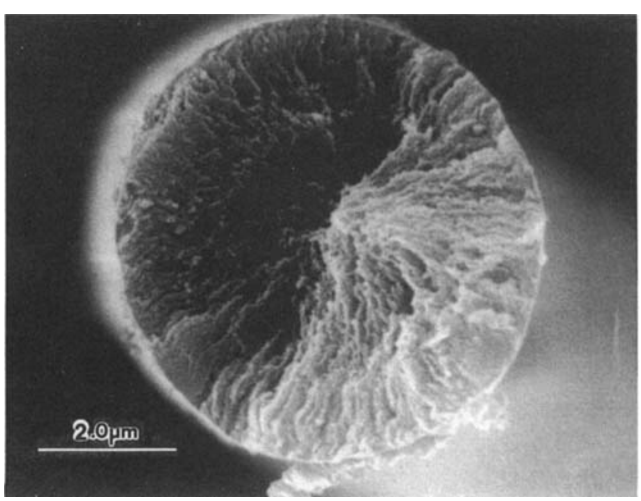

Figure 3. SEM photograph of mesophase pitch-based carbon fibre illustrating the radial texture [21].

Some degree of folding of the crystallites is also commonly observed, improving the fibres resistance to crack propagation and, thus, increasing its tensile strength. Folding is an artifact of disclinations in the precursor pitch which may, to a lesser extent, remain after spinning (if inadequate time is allowed for reorientation) [23, 24]. Fibres may also be formed with the absence of any clearly defined texture. Generation of a random texture involves complete disruption of the developing flow (for example, by spinning through capillaries containing a porous media [25]), and such fibres offer the potential of improved compressive strengths. Production of fibres with a concentric, or 'onion-skin', texture has also been reported, but it is difficult to postulate a single mechanism to explain their occurrence. Matsumoto [26] reports that extrusion through a large diameter capillary can yield fibres with a concentric texture. Hamada *et al.* [27], formed onion-skin fibres by stirring the pitch upstream from the capillary and, thus, inducing a tangential velocity component. Mochida *et al.* [28], have been able to produce fibres with a concentric texture at very high spinning temperature (low spinning viscosity). Note that the concentric texture corresponds to an in-plane director (in the absence of tangential flow).

The values $\zeta = \beta = 90°$ (corresponding to the radial orientation) can be substituted into the z-component of the conservation of linear momentum, equation (5). The simplified form is

$$\frac{\alpha_4}{2}\frac{d^2 v_z}{dr^2} + \frac{\alpha_4}{2r}\frac{dv_z}{dr} - \frac{dP}{dz} = 0. \tag{30}$$

Direct integration of equation (30) yields

$$v_z = \frac{R^2}{2\alpha_4}\left[1 - \left(\frac{r}{R}\right)^2\right]\frac{\Delta P}{L}. \tag{31}$$

The result of equation (31) is identical to the Poiseuille velocity distribution predicted for isotropic fluids, with the viscosity equal to $\alpha_4/2$. This suggests the possibility of measurement of the coefficient α_4 for a discotic material using a capillary rheometer, whenever an out-of-plane orientation can be confirmed. The velocity distribution of equation (31) is briefly mentioned by Leslie [7]; however, this form of solution has essentially been overlooked, since such out-of-plane behaviour has only rarely been observed in the extensively studied rod-like nematics. Pieranski and Guyon [29] found that a sample of rod-like p-methoxybenzilidene p-n-butylaniline (MBBA) initially oriented out of the flow–gradient plane will maintain that texture only at low velocities. Zúñiga and Leslie [30] discuss the stability of an in-plane director for a flow-aligning ($\alpha_3 < 0$) and non-flow-aligning ($\alpha_3 > 0$) rod-like nematic flowing between parallel plates using various initial boundary conditions.

It has generally been assumed that only the relative magnitudes of α_2 and α_3 are of qualitative significance in the flow of nematic liquid crystals. This assumption is based on molecular dynamics simulations predicting the viscosity of a fluid of rigid, anisotropic molecules of specific shapes [31]. Considering a fluid composed of oblate ellipsoids (disks) of a specific shape, this analysis predicted a lower viscosity with an in-plane orientation. Employing these results, Ho and Rey [32] present numerical solutions to the Leslie–Ericksen equations for the creeping flow of discotic liquid crystals between infinite converging and diverging planar walls.

However, by only considering these two coefficients, no information about the tendency for out-of-plane orientation is obtained, where the viscosity is described by α_4. In discotic systems, for instance, the above result indicates that perhaps the relative magnitudes of α_4 and K must also be considered. Also, as mentioned above, surface interactions and capillary entrance effects may influence the tendency toward stable out-of-plane orientation.

4. Channel flow

In the production of mesophase pitch-based carbon fibres, it has been found that spinning through rectangular channels yields fibres possessing a highly linear texture which is conducive to high thermal conductivity. Specifically, the resulting ribbon-shaped fibres exhibit lower electrical resistivities than circular fibres of equivalent tensile moduli (electrical resistivity is inversely related to thermal conductivity) [33]. Since stiffness is essentially a measure of axial orientation, it appears that the difference in transverse orientation is at least partially responsible for the improved conductivity.

Analysis of channel flow is somewhat more complex than capillary flow, due to the fact that there is no single gradient direction (in any convenient coordinate system), and thus, the flow is not viscometric. We may, however, begin the procedure by eliminating velocity components in the same manner as before.

$$v_x = v_y = 0. \tag{32}$$

From the conservation of mass, equation (2), the non-zero z-component of the velocity is

$$v_z = v_z(x, y). \tag{33}$$

To be perfectly general, at this point we would define the director using two angles: ζ, in the x–y plane (with respect to the x axis), and β, with respect to the flow axis. However, intuitively it is evident that there should be two solutions where the sum of torques is zero. The solution with $\beta = 90°$ seems to represent the physical situation in

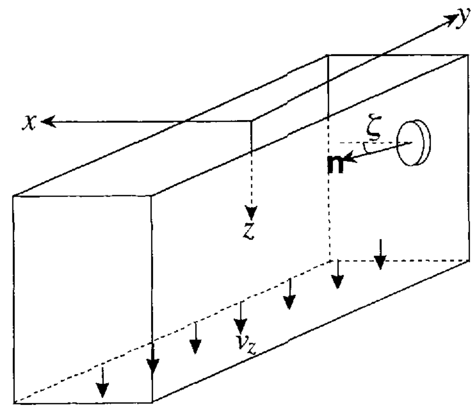

Figure 4. Director orientation angle in rectangular coordinates.

capillary flow, and the axial behaviour should be quite similar in channel flow. Therefore, due to the added complexity of this problem, we shall bypass the question of stability and assume that $\beta = 90°$, to see if the resulting predicted orientation profile qualitatively matches observed fibre textures. The out-of-plane angle, ζ, will be allowed to vary with x and y, as shown in figure 4. The director components are as follows:

$$\mathbf{n} = \begin{pmatrix} \cos\zeta(x, y) \\ \sin\zeta(x, y) \\ 0 \end{pmatrix}. \tag{34}$$

The x-, y-, and z-components of the conservation of linear momentum are

$$\frac{\partial \tau_{xx}}{\partial x} + \frac{\partial \tau_{yx}}{\partial y} + \frac{\partial \tau_{zx}}{\partial z} = 0, \tag{35}$$

$$\frac{\partial \tau_{xy}}{\partial x} + \frac{\partial \tau_{yy}}{\partial y} + \frac{\partial \tau_{zy}}{\partial z} = 0, \tag{36}$$

$$\frac{\partial \tau_{xz}}{\partial x} + \frac{\partial \tau_{yz}}{\partial y} + \frac{\partial \tau_{zz}}{\partial z} - \frac{\partial P}{\partial z} = 0. \tag{37}$$

After evaluation of the viscous stress tensor, the x- and y- components vanish, while the z-component is given by

$$\begin{aligned} &(\alpha_5 - \alpha_2)\sin(2\zeta)\left[\frac{\partial^2 v_z}{\partial x \partial y} + \frac{\partial \zeta}{\partial y}\frac{\partial v_z}{\partial y} - \frac{\partial \zeta}{\partial x}\frac{\partial v_z}{\partial x}\right] \\ &+ (\alpha_5 - \alpha_2)\cos(2\zeta)\left(\frac{\partial \zeta}{\partial x}\frac{\partial v_z}{\partial y} + \frac{\partial \zeta}{\partial y}\frac{\partial v_z}{\partial x}\right) \\ &+ [(\alpha_5 - \alpha_2)\cos^2\zeta + \alpha_4]\frac{\partial^2 v_z}{\partial x^2} \\ &+ [(\alpha_5 - \alpha_2)\sin^2\zeta + \alpha_4]\frac{\partial^2 v_z}{\partial y^2} - 2\left(\frac{dP}{dz}\right) = 0. \end{aligned} \tag{38}$$

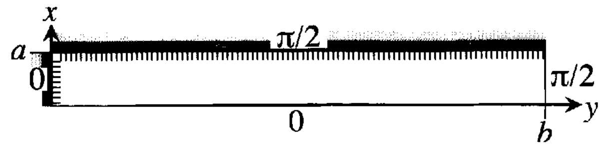

Figure 5. Director angle boundary conditions for flow through rectangular channel.

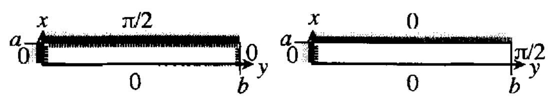

Figure 6. Partial solutions to problem represented in figure 5.

The x-, y-, and z-components of the balance of torques are

$$\frac{\partial v_z}{\partial x} = -\tan\zeta\frac{\partial v_z}{\partial y}, \quad \alpha_2 \neq 0, \tag{39}$$

$$\frac{\partial v_z}{\partial x} = -\tan\zeta\frac{\partial v_z}{\partial y}, \quad \alpha_2 \neq 0, \tag{40}$$

$$\frac{\partial^2\zeta}{\partial x^2} + \frac{\partial^2\zeta}{\partial y^2} = 0, \quad K \neq 0. \tag{41}$$

The above z-component contains only the angle, ζ, as a dependent variable. Furthermore, it takes the familiar form of the Laplace equation. Therefore, we only need to specify the appropriate boundary conditions to obtain a solution for ζ across the flow field. First, taking advantage of the symmetry of the flow system, we will consider only one quadrant from figure 4. For convenience, we will shift the origin midway along one edge. Examination of the case of flow between infinite parallel plates with an out-of-plane director (directly analogous to capillary flow) indicates that the director should tend to orient parallel to the walls of the channel. This corresponds to a perpendicular alignment of the long molecular axes with respect to the solid boundaries. The formulation of the problem is depicted in figure 5, where the dashes within the flow field represent the long molecular axes (disk edges).

The solution of equation (41) with the above boundary conditions may be obtained by superimposing solutions of similar problems, each with only one non-zero boundary condition. These problems shall be labelled Case I and Case II and are illustrated in figure 6.

The solution to the Laplace equation with boundary conditions of the form in figure 6 (a Dirichlet problem) involves a classical separation of variables technique and is summarized below.

4.1. *Case I*

By employing separation of variables, the partial differentials of equation (41) may be converted to ordinary differentials. Let

$$\zeta_{\mathrm{I}} = U(x)V(y). \tag{42}$$

The boundary conditions for Case I are

$$\zeta_{\mathrm{I}}(x,0) = 0, \tag{43}$$

$$\zeta_{\mathrm{I}}(x,\mathrm{b}) = 0, \tag{44}$$

$$\zeta_{\mathrm{I}}(0,y) = 0, \tag{45}$$

and

$$\zeta_{\mathrm{I}}(a,y) = \frac{\pi}{2}. \tag{46}$$

Using the first three boundary conditions, equations (43)–(45), the solutions for $U(x)$ and $V(y)$ are hyperbolic sine and sine functions, respectively. After recombination, the general solution for $\zeta_{\mathrm{I}}(x,y)$ is

$$\zeta_{\mathrm{I}} = \sum_{n=1}^{\infty} A_n \sinh\left(\frac{n\pi x}{b}\right)\sin\left(\frac{n\pi y}{b}\right). \tag{47}$$

The final boundary condition, equation (46), requires that

$$\sum_{n=1}^{\infty} A_n \sinh\left(\frac{n\pi a}{b}\right)\sin\left(\frac{n\pi y}{b}\right) = \frac{\pi}{2}. \tag{48}$$

The above condition, equation (48), is a Fourier sine series. Hence, the coefficients, A_n, are given by the integral

$$A_n = \frac{2}{b\sinh\left(\frac{n\pi a}{b}\right)}\int_0^b \frac{\pi}{2}\sin\left(\frac{n\pi y}{b}\right)dy = \frac{[1-(-1)^n]}{n\sinh\left(\frac{n\pi a}{b}\right)}. \tag{49}$$

Substituting these coefficients into equation (47), we obtain

$$\zeta_{\mathrm{I}} = \sum_{n=1}^{\infty} \frac{[1-(-1)^n]}{n\sinh\left(\frac{n\pi a}{b}\right)}\sinh\left(\frac{n\pi x}{b}\right)\sin\left(\frac{n\pi y}{b}\right). \tag{50}$$

4.2. *Case II*

The procedure for Case II is identical to that outlined above (with x and y interchanged). The boundary conditions are

$$\zeta_{\mathrm{II}}(x,0) = 0, \tag{51}$$

$$\zeta_{\mathrm{II}}(x,b) = \frac{\pi}{2}, \tag{52}$$

$$\zeta_{\mathrm{II}}(0,y) = 0, \tag{53}$$

and

$$\zeta_{\mathrm{II}}(a,y) = 0. \tag{54}$$

The solution for Case II is

$$\zeta_{\mathrm{II}} = \sum_{n=1}^{\infty} \frac{[1-(-1)^n]}{n\sinh\left(\frac{n\pi b}{a}\right)}\sin\left(\frac{n\pi x}{a}\right)\sinh\left(\frac{n\pi y}{a}\right). \tag{55}$$

Finally, we can generate the solution to the problem shown in figure 5 by summing equations (50) and (55). The result predicts that the orientation angle should vary across the flow field according to

$$\zeta = \sum_{n=1}^{\infty} \frac{[1-(-1)^n]}{n} \left[\frac{\sinh\left(\frac{n\pi x}{b}\right)}{\sinh\left(\frac{n\pi a}{b}\right)} \sin\left(\frac{n\pi y}{b}\right) + \frac{\sinh\left(\frac{n\pi y}{a}\right)}{\sinh\left(\frac{n\pi b}{a}\right)} \sin\left(\frac{n\pi x}{a}\right) \right], \tag{56}$$

for $0 \le x \le a$ and $0 \le y \le b$. Recall that this describes only one quadrant of the channel. However, the orientation fields of the remaining quadrants of the channel are simply mirror images of the above expression. The solutions to Cases I and II, as well as their recombination, involve fairly classical techniques treated in a number of textbooks (see, for instance, Hildebrand [34]). For the case of $b = 9a$, the orientation profile appears as shown in figure 7. This pattern bears a striking resemblance to a typical fracture surface observed in ribbon-shaped mesophase pitch-based carbon fibres when viewed under a scanning electron microscope (SEM), as shown in figure 8. These fibres were spun using a spinnerette containing 12 rectangular channels, each with a 9 : 1 aspect ratio.

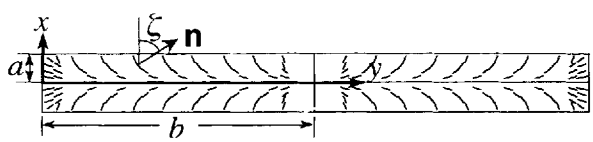

Figure 7. Transverse view of the orientation of a discotic mesophase flowing through a channel.

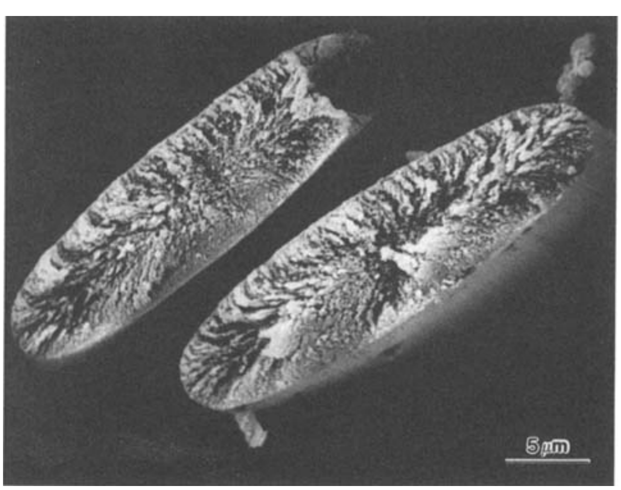

Figure 8. SEM photograph of a ribbon-shaped mesophase pitch-based carbon fibre [35].

The solution for ζ in equation (56) could be substituted into the z-component of the conservation of linear momentum, equation (38), using equations (39)/(40) to obtain the velocity profile.

5. Concluding remarks

The theory of Leslie and Ericksen has been applied to a system with a director component out of the flow–gradient plane. While this approach differs from most previous work involving solutions to the Leslie–Ericksen equations, it yields orientation profiles which agree qualitatively with the structures commonly observed in carbon fibres melt-spun from mesophase pitch, a discotic liquid crystalline material.

The agreement of the above solutions with the observed microstructures indicates that increased attention must be given to the tendency of the director to achieve a stable orientation out of the flow–gradient plane. This tendency determines the relative stability of the commonly observed radial texture versus the concentric texture in mesophase pitch-based carbon fibres.

This research is sponsored by the United States Department of the Navy, Office of Naval Research, Manufacturing Technology Program (Mr Steve Linder, technical monitor) and administered by the Great Lakes Composites Consortium (Mr Paul Harruff, contract monitor), through contract number TDL 92-09. The authors would like to thank Professor R. B. Bird, Chemical Engineering Department, University of Wisconsin, for his helpful advice.

References

[1] Singer, L. S., 1977, U.S. Patent, 4 005 183.
[2] Otani, S., Watanabe, S., Ogino, H., Iigima, K., and Koitabashi, T., 1972, *Bull. chem. Soc. Japan*, **45**, 3710.
[3] Mochida, I., Shimizu, K., Korai, Y., Otsuka, H., and Fujiyama, S., 1988, *Carbon*, **26**, 843.
[4] Brooks, J. D., and Taylor, G. H., 1968, *Chemistry and Physics of Carbon*, Vol. 4, edited by P. L. Walker, Jr. (Marcel Dekker), p. 243.
[5] Zimmer, J. E., and White, J. L., 1982, *Advances in Liquid Crystals*, Vol. 5, edited by H. G. Brown (Academic Press), p. 157.
[6] Edie, D. D., and Stoner, E. G., 1992, *Carbon–Carbon Materials and Composites*, edited by J. D. Buckley and D. D. Edie (Noyes Publications), p. 41.
[7] Leslie, F. M., 1966, *Q. Jl Mech. appl. Math.*, **19**, 357.
[8] Leslie, F. M., 1968, *Archs Ration. mech. Anal.*, **28**, 265.
[9] Ericksen, J. L., 1960, *Kolloid Z.*, **173**, 117.
[10] Ericksen, J. L., 1960, *Archs Ration. mech. Anal.*, **4**, 231.
[11] Ericksen, J. L., 1961, *Trans. Soc. Rheol.*, **5**, 23.
[12] Ericksen, J. L., 1962, *Archs Ration. mech. Anal.*, **9**, 371.
[13] Parodi, O., 1970, *J. Phys., Paris*, **31**, 581.
[14] Oseen, C. W., 1933, *Trans. Faraday Soc.*, **29**, 883.
[15] Frank., F. C., 1958, *Discuss Faraday Soc.*, **25**, 19.
[16] Atkin, R. J., 1970, *Archs Ration. mech. Anal.*, **38**, 224.

[17] TSENG, H. C., SILVER, D. L., and FINLAYSON, B. A., 1972, *Physics Fluids*, **15**, 1213.
[18] LESLIE, F. M., 1979, *Advances in Liquid Crystals*, Vol. 4, edited by H. G. Brown (Academic Press), p. 1.
[19] VOLOVIK, G. E., 1980, *JETP Lett.*, **31**, 273.
[20] CARLSSON, T., 1982, *Molec. Crystals liq. Crystals*, **89**, 57.
[21] MCHUGH, J. J., LIU, G. Z., and EDIE, D. D., 1992, *Tanso*, **155**, 417.
[22] ENDO, M., 1988, *J. mater. Sci.*, **23**, 598.
[23] BUECHLER, M., NG, C. B., and WHITE, J. L., 1983, *Extended Abstracts of the 16th Biennial Conference on Carbon.*
[24] HAMADA, T., NISHIDA, T., SAJIKI, Y., and MATSUMOTO, M., 1987, *J. mater. Res.*, **2**, 850.
[25] NAZEM, F., 1983, U.S. Patent, 4 376 747.
[26] MATSUMOTO, T., 1985, *Pure appl. Chem.*, **57**, 1553.
[27] HAMADA, T., NISHIDA, T., FURUYAMA, M., and TOMIOKA, T., 1988, *Carbon*, **26**, 837.
[28] MOCHIDA, I., YOON, S. H., and KORAI, Y., 1993, *J. mater. Sci.*, **28**, 2331.
[29] PIERANSKI, P., and GUYON, E., 1973, *Sol. St. Commun.*, **13**, 435.
[30] ZÚÑIGA, I., and LESLIE, F. M., 1989, *J. Non-Newton. Fluid Mech.*, **33**, 123.
[31] SOLLICH, H., BAALSS, D., and HESS, S., 1989, *Molec. Crystals liq. Crystals*, **168**, 189.
[32] HO, A. S. K., and REY, A. D., 1991, *Rheol. Acta*, **30**, 77.
[33] ROBINSON, K. E., ROGERS, D. K., MCHUGH, J. J., EDIE, D. D., and FAIN, C. C., 1992, *Carbon '92: Proceedings of the 5th International Conference on Carbon*, Essen, Germany, p. 816.
[34] HILDEBRAND, F. B., 1976, *Advanced Calculus for Applications* (Prentice-Hall).
[35] EDIE, D. D., ROBINSON, K. E., FLEUROT, O., JONES, S. P., and FAIN, C. C., 1994, *Carbon*, **32**, 1045.